



Article

An Artificial Intelligence-Powered Environmental Control System for Resilient and Efficient Greenhouse Farming

Meng-Hsin Lee ¹, Ming-Hwi Yao ^{2,*}, Pu-Yun Kow ¹, Bo-Jein Kuo ³ and Fi-John Chang ^{1,*}

¹ Department of Bioenvironmental Systems Engineering, National Taiwan University, Taipei 106216, Taiwan; d07622003@ntu.edu.tw (M.-H.L.); d09622001@ntu.edu.tw (P.-Y.K.)

² Agricultural Engineering Division, Taiwan Agricultural Research Institute, Ministry of Agriculture, Taichung City 413008, Taiwan

³ Department of Agronomy, National Chung Hsing University, Taichung City 402202, Taiwan; bjkuo@nchu.edu.tw

* Correspondence: mhyao@tari.gov.tw (M.-H.Y.); changfj@ntu.edu.tw (F.-J.C.)

Abstract: The rise in extreme weather events due to climate change challenges the balance of supply and demand for high-quality agricultural products. In Taiwan, greenhouse cultivation, a key agricultural method, faces increasing summer temperatures and higher operational costs. This study presents the innovative AI-powered greenhouse environmental control system (AI-GECS), which integrates customized gridded weather forecasts, microclimate forecasts, crop physiological indicators, and automated greenhouse operations. This system utilizes a Multi-Model Super Ensemble (MMSE) forecasting framework to generate accurate hourly gridded weather forecasts. Building upon these forecasts, combined with real-time in-greenhouse meteorological data, the AI-GECS employs a hybrid deep learning model, CLSTM-CNN-BP, to project the greenhouse's microclimate on an hourly basis. This predictive capability allows for the assessment of crop physiological indicators within the anticipated microclimate, thereby enabling preemptive adjustments to cooling systems to mitigate adverse conditions. All processes run on a cloud-based platform, automating operations for enhanced environmental control. The AI-GECS was tested in an experimental greenhouse at the Taiwan Agricultural Research Institute, showing strong alignment with greenhouse management needs. This system offers a resource-efficient, labor-saving solution, fusing microclimate forecasts with crop models to support sustainable agriculture. This study represents critical advancements in greenhouse automation, addressing the agricultural challenges of climate variability.



Citation: Lee, M.-H.; Yao, M.-H.; Kow, P.-Y.; Kuo, B.-J.; Chang, F.-J. An Artificial Intelligence-Powered Environmental Control System for Resilient and Efficient Greenhouse Farming. *Sustainability* **2024**, *16*, 10958. <https://doi.org/10.3390/su162410958>

Academic Editor: Sean Clark

Received: 11 November 2024

Revised: 10 December 2024

Accepted: 12 December 2024

Published: 13 December 2024



Copyright: © 2024 by the authors. Licensee MDPI, Basel, Switzerland. This article is an open access article distributed under the terms and conditions of the Creative Commons Attribution (CC BY) license (<https://creativecommons.org/licenses/by/4.0/>).

1. Introduction

In the past two decades, the frequency and intensity of extreme weather events have accelerated the global water cycle, resulting in more severe droughts and floods [1]. Such climate changes are having increasing impacts on agriculture worldwide and pose significant challenges to food systems, e.g., crop loss and food insufficiency [2]. The Institute for Economics and Peace (IEP) warns that climate change is not only driving food insecurity but also causing displacement, pressing affected populations to face harsh new realities [3]. Extreme weather conditions, such as strong winds and heavy rains, can devastate agricultural production, sometimes wiping out an entire season's harvest. As the demand for high-quality, safe agricultural products continues to grow, precise and resilient crop management strategies have become essential [4].

Precision agriculture has emerged as a vital strategy to prevent crop loss and enhance production on limited land, particularly in the face of climate change and natural disasters [5,6]. By providing precise irrigation, fertilization, and environmental management, precision agriculture helps mitigate the impact of natural disasters and supports

optimal crop growth. Therefore, greenhouses have become a prominent setting for implementing precision agriculture due to their controlled environment, which shields crops from adverse local climate conditions that can hinder growth [3]. Advanced technologies, such as the Internet of Things (IoT), cloud-based servers, and Artificial Intelligence (AI), have further accelerated the adoption of precision agriculture within greenhouses. These innovations enable precise regulation of critical factors like temperature and humidity, significantly boosting agricultural productivity.

In response to changing climates, unpredictable weather, and rising demand, greenhouse cultivation is increasingly critical for stabilizing crop prices and ensuring food security by providing controlled environments for reliable crop production. Globally, greenhouse cultivation now spans approximately 405,000 hectares [7,8]. Modern greenhouses not only protect crops from external threats like rain, wind, high and low temperatures, and pests, but they also actively control internal conditions, enabling high yields, improved crop quality, and efficient water use [9,10]. In recent years, the development of climate-smart greenhouses has centered on the advancement of environmental sensors and IoT technologies [11]. While different greenhouse types aim to create optimal microclimates, there is a growing need to forecast microclimate conditions within greenhouses to better support crop management [2,12,13]. Many structural greenhouses are already equipped with environmental control systems designed to adjust internal conditions, such as activating shading nets or cooling systems when temperatures exceed certain thresholds [14,15]. These control systems are often integrated with information and communication techniques, enabling farmers to monitor conditions and operate equipment remotely via mobile applications. However, the effective operation of climate-smart greenhouses relies heavily on numerous sensors throughout the structure [16,17]. The durability of these sensors is challenged by the high-temperature, high-humidity environment, which often leads to frequent malfunctions, increased maintenance costs, and limited repair options, which ultimately hinder the efficiency of greenhouse automation.

Predicting and managing greenhouse microclimates is challenging due to the complex dynamics of heat transfer within these controlled environments [18–20]. Effective environmental management is essential to cultivating crops under optimal microclimate conditions [21,22], influenced by key factors such as temperature, relative humidity, and photosynthetically active radiation [23,24]. For instance, maintaining appropriate relative humidity is vital for crop growth, impacting both crop quality and dehumidification costs [25]. Manual cooling is often needed to regulate internal temperatures, ensuring conditions that support optimal crop physiology [26]. In addition, adequate ventilation is crucial for temperature control, as greenhouse operations play a significant role in mediating the heat exchange with the external environment [2,25,27]. Another key aspect of greenhouse management is the integration of atmospheric weather forecasts to inform predictive models for greenhouse microclimates [3]. Atmospheric grid forecast points could provide localized information relevant to greenhouses in specific regions, and the forecast lead time is essential for assessing the applicability of these predictions in greenhouse settings. In Taiwan, however, current agricultural weather forecasts, which are updated every three hours and lack light intensity data, are insufficient for the demands of climate-smart greenhouse management.

Over time, greenhouse systems have evolved from basic environmental controls that respond to internal conditions to advanced, intelligent systems powered by AI. Among AI approaches, deep learning techniques excel in extracting meaningful patterns from complex datasets, making them particularly suited for modeling the nonlinear systems typical of greenhouse environments. These techniques are valued for their ability to produce reliable outputs by learning from historical data [28,29] and continue to play a key role in greenhouse modeling [30–32]. For instance, modeling greenhouse microclimates requires capturing intricate dependencies between external and internal weather conditions, a challenge addressed by various methods, including backpropagation neural networks (BPNNs), adaptive network-based fuzzy inference systems (ANFISs), and support vector

regression (SVM) [2,33–36]. Advances in cloud computing and IoT devices have further enabled the integration of greenhouse microclimate, irrigation, and crop growth regulation with AI algorithms [37,38]. This integration allows for continuous monitoring, recording, and analysis of the relationships between crop growth and environmental factors. Combining automated control systems with AI-driven decision-making, the development of “Autonomous Greenhouses” is underway [30,39,40], aiming to reduce water and fertilizer use, save labor, and increase yields simultaneously.

Taiwan, which comprises tropical and subtropical regions, excels not only in advanced agricultural practices but also in greenhouse construction technology and information and communication technology (ICT) capabilities [15,41]. Leveraging these strengths to build a globally competitive facility-based agriculture sector is a key focus for agricultural research and development (R&D). In response to changing meteorological conditions and labor shortages, enhancing greenhouse automation is essential to reduce manual labor and improve efficiency. Achieving this requires the digitalization of diverse crop and environmental data within greenhouses, alongside the integration of AI to address existing cultivation challenges. This study aims to develop an innovative AI-powered greenhouse environmental control system (AI-GECS), which consists of four primary modules: (1) a short-term gridded weather forecast module, (2) an internal microclimate forecast module, (3) a crop physiological indicators module, and (4) an AI-enabled environmental control module. An experimental greenhouse for tomato (*Solanum lycopersicum* L.) cultivation, located at the Taiwan Agricultural Research Institute (TARI), will serve as the case study to test this system. The AI-GECS is designed to optimize greenhouse conditions autonomously, reducing water and resource usage, alleviating labor demands, and ultimately enhancing productivity and crop quality in a controlled environment.

2. Materials and Methods

2.1. Experiment Site and Materials

This study utilizes datasets from a greenhouse located at the TARI in Central Taiwan (Figure 1).

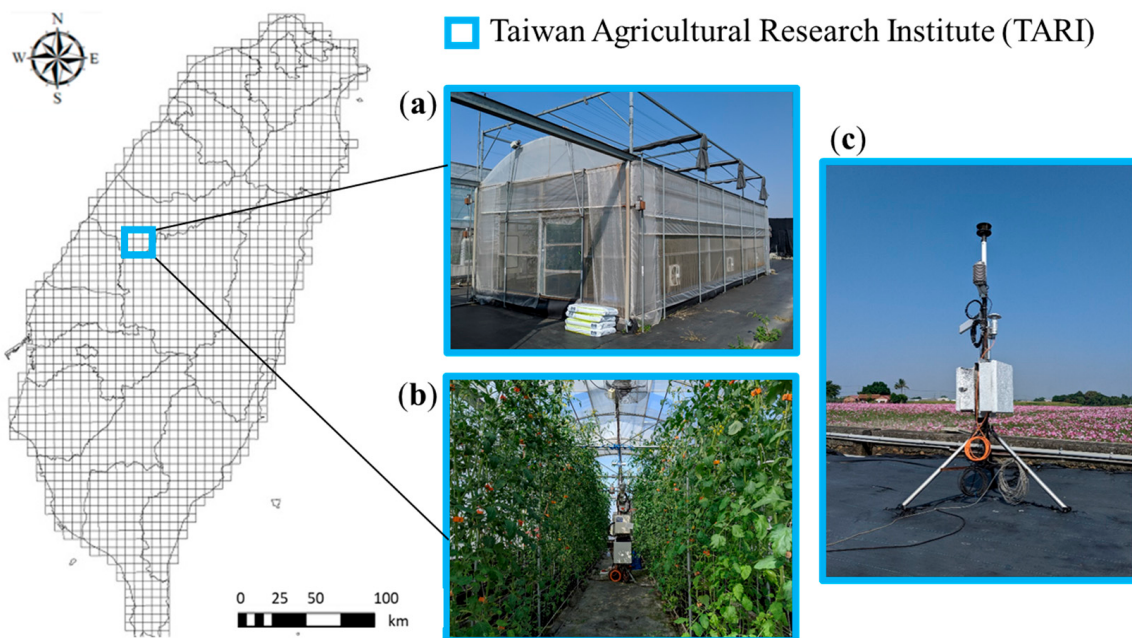


Figure 1. Illustration of the study area located in the Taiwan Agricultural Research Institute (TARI) in Central Taiwan. (a) TARI greenhouse. (b) Tomato cultivation. (c) Outdoor weather monitoring station.

The greenhouse measures 12 m × 5 m × 4.3 m and is covered with a 0.18 mm thick plastic film. It is equipped with an external shading net on the roof, two rolling plastic

films that open the roof skylights, and four perimeter rolling plastic films, each of which are independently motorized and integrated with the greenhouse control system. To monitor the internal microclimate, IoT sensors installed within the greenhouse include a temperature and humidity sensor (HMP60, Vaisala, Vantaa, Finland), a quantum sensor (SQ-215, Apogee Instruments, UT, USA), and a carbon dioxide sensor (GMP343, Vaisala, Finland). An outdoor weather monitoring station equipped with the same types of sensors as those inside the greenhouse, along with a two-dimensional sonic wind sensor (WindSonic 1405-PK-100, Gill Instruments, Hampshire, UK), provide data on the external microclimate. All meteorological data are logged every 10 min using a data logger (CR1000, Campbell Scientific, UT, USA).

2.2. Methods

This study introduces an AI-powered greenhouse environmental control system (AI-GECS) that integrates customized gridded weather forecasts, AI-based microclimate forecasts, a crop physiological indicator, and greenhouse operation strategies (Figure 2).

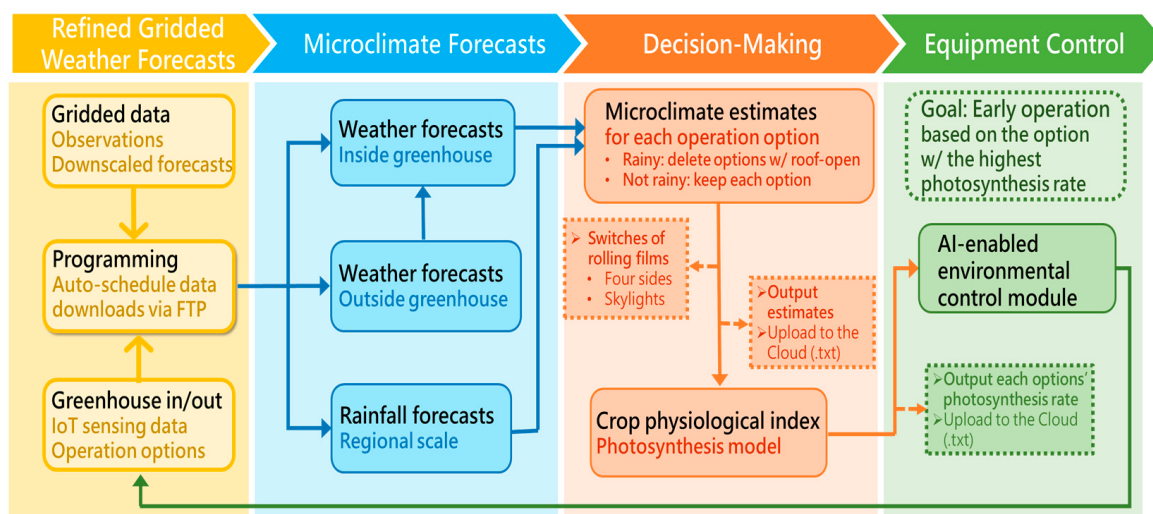


Figure 2. Conceptual flow of the proposed AI-powered greenhouse environmental control system (AI-GECS).

The AI-GECS aims to enhance greenhouse environmental control by refining 3 h gridded weather forecasts to an hourly resolution, generating hourly internal microclimate forecasts using AI techniques based on these refined weather forecasts, and applying hourly environmental controls guided by microclimate forecasts and optimized crop growth indicators. The methods employed in this study are outlined below.

2.3. Short-Term Gridded Weather Forecast Module: Multi-Model Super-Ensemble Forecasting (MMSE)

This study develops a Multi-Model Super Ensemble (MMSE) forecasting system that combines the Temporal and Spatial Mesoscale Analysis System–Weather Research and Forecasting (STMAS-WRF) methods with weather station data and applies the Inverse Distance Weighted (IDW) downscaling technique (STMAS-WRF-IDW) to generate hourly gridded weather forecasts. The resulting $3 \times 3 \text{ km}^2$ gridded forecasts deliver hourly updates on key meteorological variables, including temperature (Temp), relative humidity (RH), short-wave radiation (SWR), longwave radiation (LWR), vapor pressure deficit (VPD), dew point temperature (DSF), and sea-level pressure (SLP), among others. STMAS decomposes observational data, preserving weather characteristics across different wavelengths on a 3 km grid, while WRF generates gridded weather forecast data [42]. The IDW method [43,44] is then used to map these gridded forecasts to the specific coordinates of the TARI greenhouse,

creating highly localized weather forecasts. In addition, an ensemble of forecasts from two machine learning models produces hourly gridded rainfall forecasts.

The MMSE utilizes a time-delay approach to generate multiple forecast sets for the same horizon, effectively simulating multi-model forecasts and matching them with observational data to train the ensemble system (Figure 3).

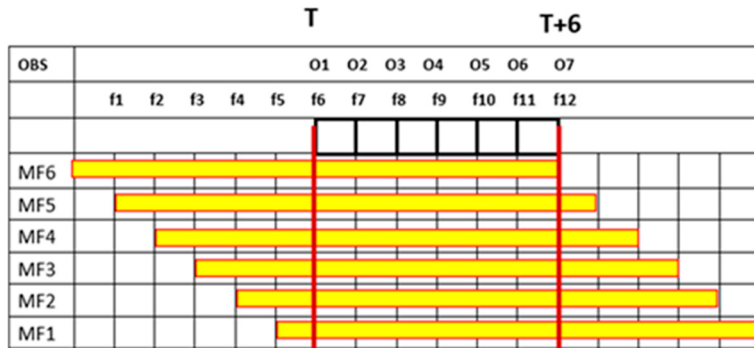


Figure 3. Conceptual illustration of the time-delay method for multi-model super-ensemble forecasting. MF1-MF6 denote six forecast models.

Once trained, the MMSE applies the learned weights to each forecast sample, resulting in enhanced forecast values. The process of determining these weights involves using the historical forecasts of each sample, observational data, and climatological data. For each grid, the weight of individual forecast model for each sample is calculated, and the gridded forecasts are then produced according to the following forecast method based on [45], shown as follows:

$$S_b = \overline{O_b} + \sum_{i=1}^{N_{mdl}} a_{b,i} + (F_{b,i} - \overline{F}_{b,i}) \quad (1)$$

where S_b represents the forecast value, $\overline{O_b}$ represents the average of the observed data, calculated as the average over the training period, $F_{b,i}$ is the forecast value of model i at grid b , and $\overline{F}_{b,i}$ is the average of model i at grid b , also taken as the average over the training period. The weight $a_{b,i}$ is calculated based on the data in the training period. N_{mdl} denotes the total number of models for the ensemble.

This method illustrates the advantages and implications of the multi-model regression method. It shows that the model adjusts weights based on the minor differences in the model's systematic errors ($F_{b,i} - \overline{F}_{b,i}$), resulting in an improved error distribution. Then, it combines the adjusted weights to generate a new forecast. The weights are obtained using the Root Mean Square Error minimization method, as expressed in Equation (2):

$$G = \sum_{t=1}^{N_{train}} (S_t - O_t) \quad (2)$$

where G denotes the total error, S_t represents the forecast value, O_t represents the observed value, and N_{train} denotes the total time horizons in the training period. The goal is to reach $G = 0$, i.e., no error.

The study aims to generate up-to-date hourly gridded forecast data tailored for greenhouse operations. Recognizing that the length of training data and varying data durations significantly impact both the computational resources and processing time required for super-ensemble forecasting, this study focuses on evaluating the optimal training data length. By assessing the benefits of different data durations, this study seeks to enhance forecast accuracy while optimizing computational efficiency.

2.4. Microclimate Forecast Module: CLSTM-CNN-BP

Reducing reliance on IoT devices can significantly enhance climate-smart greenhouse farming by alleviating the financial burden and labor cost on greenhouse owners. To

facilitate this transition, this study proposes substituting IoT data with open-source datasets, such as gridded weather forecast data. By configuring a hybrid multi-factor deep learning network, this module effectively processes two data sources—the gridded dataset and the greenhouse control dataset—to generate multi-factor, multi-step-ahead forecasts of internal microclimate conditions.

In this framework, the greenhouse control dataset is utilized as input for a physics-based model to simulate internal greenhouse temperatures. The study develops the CLSTM-CNN-BP model, which integrates two deep neural networks: the Convolutional Long Short-Term Memory (CLSTM) network and the Convolutional Neural Network (CNN), alongside a regression Backpropagation Neural Network (BPNN). This hybrid model forecasts three microclimate variables that significantly affect crop growth, including Temp, RH, and PAR (Figure 4). By leveraging advanced deep learning techniques, the CLSTM-CNN-BP model efficiently extracts essential features from high-dimensional data, significantly improving forecast accuracy and reliability.

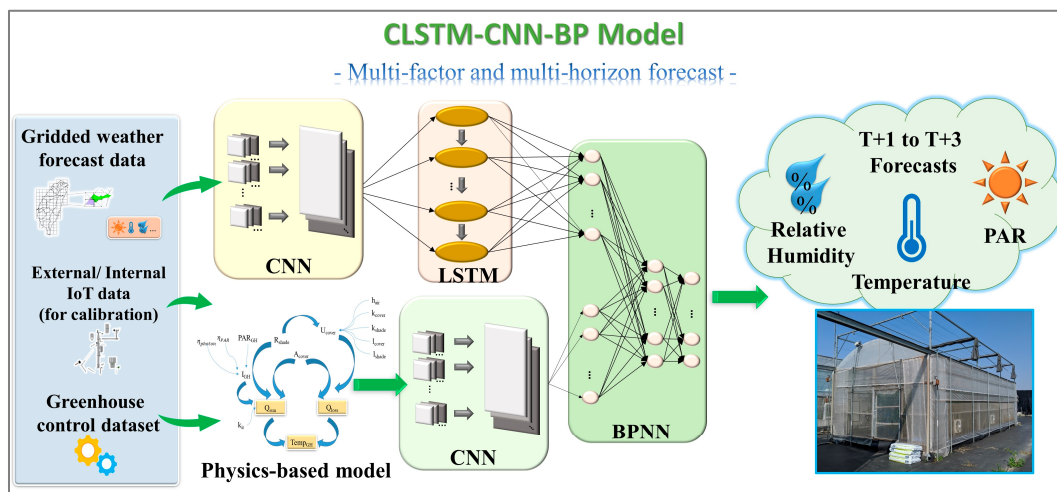


Figure 4. Architecture of the CLSTM-CNN-BP model.

The model combines CLSTM and CNN to handle multiple heterogeneous inputs: the gridded weather forecast dataset (including Temp, RH, PAR, DSF, VPD, SLP, LWR, and PSF) is processed by CLSTM, while simulated data of internal greenhouse temperature from a physics-based model is fed into CNN. The goal is to make 3 h-ahead forecasts in 10 min increments (i.e., $t + 1$ to $t + 18$) for the greenhouses. Typically, 1 h-ahead microclimate forecasts ($t + 6$) are sufficient for farmers to optimize greenhouse control. However, due to frequent delays in the gridded weather forecast data transmission, providing 2- or 3 h-ahead forecasts is essential for timely greenhouse environment management.

2.4.1. Convolutional Neural Network (CNN)

CNN is widely used for image recognition, effectively identifying key objects through its filtering mechanism [22,46,47]. This study highlights the use of CNN to extract key temporal features and denoise time series data. Typically, a CNN consists of a convolutional layer to extract important features, a max-pooling layer to reduce dimensions while preserving key information, and a fully connected layer to reshape the output into a one-dimensional vector. However, the max-pooling layer is excluded here due to its potential to eliminate essential information, negatively impacting forecast accuracy.

2.4.2. Long Short-Term Memory Neural Network (LSTM)

LSTM is a well-known recurrent neural network (RNN) in deep learning [48,49]. Unlike traditional RNNs, which only have short-term memory, LSTMs address this limitation by incorporating long-term memory. An LSTM consists of a memory cell and three gates: the input gate, the output gate, and the forget gate. The memory cell retains the output

value for use in subsequent cells. The input gate determines how much of the current input information to store in the memory cell. The output gate controls the information that is produced as output. The forget gate decides what information to discard.

2.4.3. Physics-Based Model

This study implements a physics-based model incorporating external greenhouse Temp and the greenhouse control configurations to simulate internal greenhouse Temp. The mathematical formula for simulating internal Temp is presented below, with further details available in [50]:

$$Temp_{int,T+1} = \frac{k_{ir}Q_{sun}S_i - Q_{loss}S_i}{\rho_{air}V_{air}c_{air}} + Temp_{int,T} (K) \quad (3)$$

where k_{ir} denotes the scale for converting solar radiation to sensible heat; Q_{sun} denotes the solar radiation; Q_{loss} denotes the heat dissipation; S_i (unit : m^2) denotes the shaded area of the i th control devices in the greenhouse; ρ_{air} (unit : kg/m^3) denotes the air density; V_{air} (unit : m^3) denotes the total air volume in the greenhouse; and c_{air} (unit : $kJ/kg \cdot K$) denotes the isobaric specific heat capacity.

2.5. Crop Physiological Indicator Module: Photosynthesis Rate

This study adopts the photosynthesis model proposed by [51–53], shown as follows.

$$P_{leaf} = \left\{ Q_E \cdot PAR + P_{max} - \sqrt{\left[(Q_E \cdot PFD + P_{max})^2 - 4\Theta \cdot Q_E \cdot PFD \cdot P_{max} \right]} \right\} / 2\Theta \quad (4)$$

where P_{leaf} denotes the leaf photosynthesis rate, Q_E denotes the quantum efficiency, PAR denotes the photosynthetically active radiation, P_{max} denotes the maximal leaf photosynthesis rate, PFD denotes the photon flux density, and Θ is a constant (set as 0.7, [54]). More details about the photosynthesis model can be found in [51].

It is noted that the suitable cultivation condition for tomatoes in the study area would be 20–32 °C for Temp, 40–80% for RH, and 600–1000 $\mu mol \cdot m^{-2} \cdot s^{-1}$.

2.6. AI-Enabled Environment Control Module

The AI-enabled environmental control module developed in this study incorporates microclimate forecast data into a leaf photosynthesis model to identify the optimal combination that maximizes the photosynthesis rate (Figure 5). This module processes computational results from a remote server, which informs greenhouse operational decisions for the upcoming hour, such as adjusting fans, rolling plastic films, and deploying shading nets. Unlike traditional models, this innovative module offers the advantage of hourly dynamic adjustments to greenhouse operations, enhancing responsiveness and optimizing environmental conditions for crop growth.

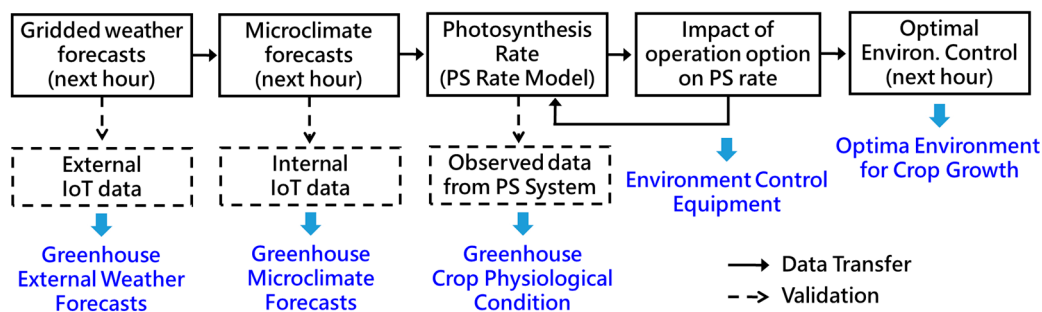


Figure 5. Illustration of the data flow for the AI-enabled environment control module.

2.7. Evaluation Metrics

The statistical metrics selected to evaluate model performance are the Root Mean Square Error (RMSE) and the Coefficient of Determination (R^2).

$$RMSE = \sqrt{\frac{\sum_{t=1}^N (O_t - S_t)^2}{N}} \quad (5)$$

$$R^2 = 1 - \frac{\sum_{t=1}^N (O_t - S_t)^2}{\sum_{t=1}^N (O_t - \bar{O})^2} \quad (6)$$

where N represents the data length, O_t represents the observed data, S_t represents the forecast values, and \bar{O} is the mean of the observed data.

3. Results

Taiwan is rich in meteorological resources; however, there is currently no internal microclimate forecasting service specifically designed for greenhouses. To fill this gap, this study develops an AI-powered greenhouse environmental control system (AI-GECS), integrating climate-smart agriculture and IoT technologies to address existing challenges in greenhouse environmental management. The system utilizes external gridded weather data to forecast the internal microclimate of the greenhouse. These microclimate forecast data are subsequently integrated with a photosynthesis model to generate optimal environmental control strategies. All data processing occurs in the cloud, requiring only a device to receive control commands and a connector to backend control machinery within the greenhouse. This configuration significantly reduces the dependence on sensors and their associated maintenance needs. Moreover, the forecasting capability facilitates proactive control adjustments, enabling the mitigation of adverse growth conditions for crops. The findings of this study are presented below.

3.1. Development of the AI-Powered Greenhouse Environmental Control System (AI-GECS)

The control process of the AI-GECS consists of five steps (Figure 6), each of which is validated with corresponding observed data.

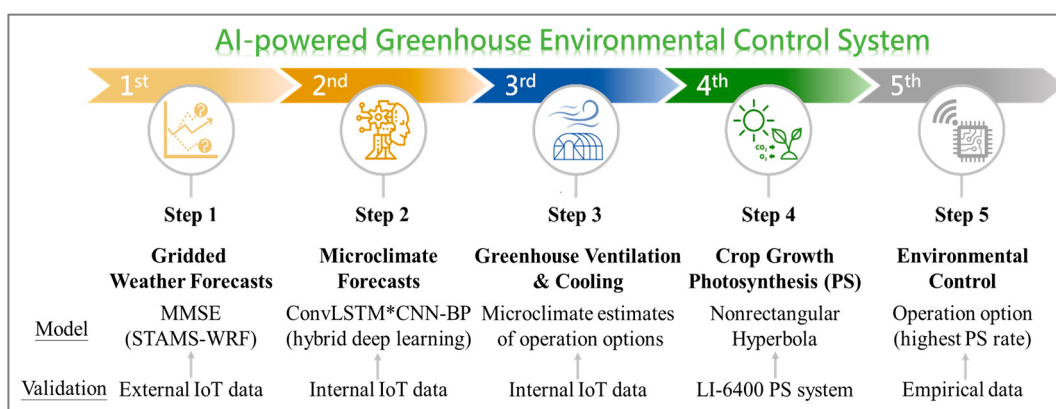


Figure 6. Control process of the AI-powered greenhouse environmental control system (AI-GECS).

Step 1: Refined Gridded Weather Forecasts for the Greenhouse

The MMSE generates 3×3 km gridded hourly weather forecasts for the next 12 h, providing vital environmental parameters outside the greenhouse, including Temp, RH, SWR, LWR, VPD, DSF, and SLP.

Step 2: Microclimate Forecasts within the Greenhouse

Using the gridded forecast data (Temp, RH, and SWR measured in W/m^2), the CLSTM-CNN-BP model generates internal microclimate forecasts for the next hour, which

include Temp, RH, and PAR. In addition, gridded rainfall forecasts help determine whether the greenhouse roof should be closed in the next hour.

Step 3: Impact of Environmental Control Equipment on Microclimate

Based on the microclimate forecast for the next hour, the microclimate model simulates the effects of various operational combinations of environmental control equipment (such as fans, rolling plastic films, and shading nets) on internal climate conditions. Each combination produces a distinct microclimate estimate.

Step 4: Photosynthesis Model

The microclimate estimates generated are input into the photosynthesis model to identify the equipment combination that yields the highest photosynthesis rate. This combination signifies the optimal growth conditions for the tomatoes and serves as a guide for environmental control in the upcoming hour.

Step 5: AI-enabled Greenhouse Environmental Control Module

All calculations are performed on a remote server, and operational instructions are transmitted to the greenhouse control module via a 4G network. The environmental control module receives directives for optimal management of greenhouse conditions in the next hour, ensuring the best possible growing environment.

This dynamic control process operates hourly, enabling the system to proactively initiate cooling or rain protection measures, which enhances conditions for crop growth.

3.2. Refined Gridded Weather Forecasts for the Greenhouse

In this study, we produce hourly $3 \times 3 \text{ km}^2$ gridded weather forecasts for 2 m ground Temp, RH, and accumulated hourly solar irradiation for the TARI greenhouse using the MMSE forecast system. This system was developed based on STMAS-WRF-IDW techniques and incorporated forecast data from weather stations. The performance of the MMSE is summarized in Table 1, where MXX (24, 48, 72) indicates forecasts generated by MMSE members trained on historical data from the previous 24, 48, and 72 h, respectively. FM represents the mean of the original forecasts from the MMSE members, while MF1 denotes the forecast from the STMAS-WRF-IDW model that is closest to the target forecast time.

Table 1. Comparison of weather forecast performance in absolute error between the MMSE system and the STMAS-WRF-IDW model (March–May, 2021).

Item	Forecast Performance in Absolute Error (Forecast–Observation)				
2 m ground temperature (°C)	<1 °C M24 ¹ M48 FM MF1	49.32% ² 48.78% 26.27% 25.45%	<2 °C 80.03% 78.53% 51.99% 52.17%	<3 °C 93.39% 92.66% 74.68% 73.14%	>4 °C 1.99% 2.08% 9.60% 10.55%
RH (%)	<5% M24 M48 FM MF1	44.97% 43.57% 29.35% 23.78%	<10% 77.49% 75.63% 55.03% 46.15%	<15% 92.75% 91.67% 73.55% 65.72%	>20% 1.86% 2.04% 13.41% 18.39%
Accumulated hourly solar irradiation (MJ/m^2)	<0.25 MJ/m^2 F1-FM-M24 F1-FM-M48 F1-FM-M72 FM MF1	54.62% 54.12% 53.31% 56.34% 56.93%	<0.5 MJ/m^2 68.57% 67.26% 67.39% 67.98% 67.44%	<1 MJ/m^2 87.59% 87.27% 87.55% 86.41% 84.87%	>1.5 MJ/m^2 3.76% 3.17% 3.03% 3.94% 5.25%

¹ MXX (24, 48, 72) denotes forecasts generated by MMSE members trained on historical data from the preceding 24, 48, and 72 h, respectively. FM represents the mean of the original forecasts from MMSE members. MF1 indicates the forecast from the STMAS-WRF-IDW model that is the nearest to the forecast target time. F1-FM-MXX represents the arithmetic mean of the original forecast from the MMSE member closest to the forecast target time (F1), FM, and MXX. ² Ratio of forecasts with an absolute error (forecast–observation) < the defined value to the total number of forecasts.

Due to the characteristic zero values obtained for cumulative hourly solar radiation at night, training durations of 6 or 12 h are inadequate for obtaining non-zero training samples.

Therefore, MMSE members utilized historical data from the preceding 24, 48, and 72 h to produce cumulative hourly solar radiation forecasts. To enhance the forecast accuracy, an arithmetic average of three MMSE products was calculated to create a new cumulative hourly solar radiation forecast. For instance, F1-FM-M24 represents the arithmetic mean of the original forecast from the MMSE member closest to the target time (F1), the average of the original forecasts from all MMSE members (FM), and the model trained on the preceding 24 h of historical data (M24).

The results demonstrate that for 2 m ground temperature, the M24 model increased the proportion of forecasts with an error less than 2 °C from 52.17% to 80.03%, and those with an error less than 3 °C from 73.14% to 93.39%. For RH, the M24 model improved the proportion of forecasts with an error less than 10% from 46.15% to 77.49%, and those with an error less than 15% from 65.72% to 92.75%. When applying F1-MF-M24 for cumulative hourly solar radiation, the proportion of forecasts with an error less than 0.5 MJ/m² rose from 67.44% to 68.57%, and those with an error less than 1.0 MJ/m² increased from 84.87% to 87.59%.

It is noted that M24 also significantly reduced the percentage of large errors: forecasts for 2 m ground temperature with errors greater than 4 °C dropped from 10.55% to 1.99%, RH errors exceeding 20% decreased from 18.39% to 1.86%, and over-forecasted cumulative hourly solar radiation with errors greater than 1.5 MJ/m² reduced from 5.25% to 3.76%. These findings indicate the feasibility and practicality of utilizing gridded weather forecast data, which demonstrate acceptable error values, to enhance greenhouse microclimate forecasting.

3.3. Microclimate Forecasts Within the Greenhouse

Forecasting the microclimate within greenhouses is essential for the effective operation of climate-smart greenhouses. Early warning systems can activate relevant environmental control equipment, helping to mitigate adverse conditions that may hinder crop growth. However, due to the generally small size and structural diversity of greenhouses, creating a standardized microclimate forecast model is impractical, as microclimates are influenced by local meteorological conditions and atmospheric circulation patterns. This study unites atmospheric experts from various domains to adapt existing gridded weather forecast services through both spatial and temporal downscaling. By integrating these gridded forecasts with actual greenhouse meteorological observations and leveraging AI technology, we establish a greenhouse-specific microclimate forecast model in consideration of (a) the impact of environmental control equipment on microclimate and (b) the photosynthesis rate.

3.3.1. Impact of Environmental Control Equipment on Microclimate and Photosynthesis Rate

Table 2 shows the opening areas of various equipment configurations with the Temp difference between the inside and outside of the greenhouse. This study also establishes a relationship between the opening area and the Temp difference (Equation (7)) and estimates the greenhouse's internal Temp conditions (Equation (8)). Furthermore, the microclimate effects of each opening area are incorporated into the photosynthesis model to determine the configuration that maximizes photosynthesis rate.

$$\text{Temp difference } (\text{°C}) = -5.7743 \times \text{percentage of opening area } (\%) + 10.558 \quad (7)$$

$$\text{Internal Temp } (\text{°C}) = \text{External Temp } (\text{°C}) + \text{Temp difference } (\text{°C}) \quad (8)$$

Table 2. Opening areas of various equipment configurations and the corresponding temperature difference between the inside and outside of the greenhouse.

Equipment Configurations	Percentage of Opening Area (%)	Temperature (Temp) Difference (°C)
Fully open	100.0	5.0 ± 0.6
Open plastic films around the perimeter	63.0	5.5 ± 0.5
Open roof skylights	37.0	9.3 ± 2.5

Table 2. Cont.

Equipment Configurations	Percentage of Opening Area (%)	Temperature (Temp) Difference (°C)
Open plastic films on right and left sides	44.4	9.0 ± 1.1
Open plastic films on front and back sides	18.4	9.0 ± 1.0
Open roof skylights and plastic films on right and left sides	81.4	5.5 ± 0.8
Open roof skylights and plastic films on front and back sides	55.5	8.0 ± 0.3
Open plastic films on the right side	22.2	8.4 ± 1.9
Open plastic films on the back side	9.3	10.3 ± 0.0

3.3.2. Microclimate Forecasting

This study presents a hybrid deep learning model (CLSTM-CNN-BP) to provide accurate greenhouse microclimate forecasts (Temp, RH, and PAR) for the coming three hours without relying on costly IoT devices. The model integrates a convolutional-based LSTM, CNN, and BPNN and uses gridded weather data and simulated greenhouse temperatures in consideration of the environmental control equipment configuration that achieves the highest photosynthesis rate. The model construction combined gridded 6 h-ahead hourly weather forecasts from the MMSE with 3 h-ahead greenhouse internal temperature simulations generated by a physics-based model at a 10 min resolution. A deep learning model fusing CNN, LSTM, stacked LSTM, and BPNN (CNN-LSTM-SLSTM-BP) that includes the greenhouse's external IoT data forms the comparative model.

Table 3 shows the test performances of CLSTM-CNN-BP and CNN-LSTM-SLSTM-BP for microclimate forecasts in the TARI greenhouse at horizons T + 1 through T + 3.

Table 3. Forecast performance of greenhouse microclimate (Temp, RH and PAR) based on the test dataset at horizons T + 1 up to T + 3 for the TARI greenhouse.

Factor	Horizon	Coefficient of Determination (R^2)		Root Mean Square Error (RMSE)	
		CLSTM-CNN-BP	CNN-LSTM-SLSTM-BP	CLSTM-CNN-BP	CNN-LSTM-SLSTM-BP
Temp (°C)	T + 1 ¹	0.69 (15.00) ⁴	0.60	5.30 (10.47) ⁴	5.92
	T + 2 ²	0.67 (11.67)	0.60	5.35 (10.08)	5.95
	T + 3 ³	0.63 (16.67)	0.54	5.45 (13.90)	6.33
RH (%)	T + 1	0.76 (-5.00)	0.80	0.14 (-16.67)	0.12
	T + 2	0.71 (-8.97)	0.78	0.16 (-33.33)	0.12
	T + 3	0.65 (-5.80)	0.69	0.16 (-14.29)	0.14
PAR ($\mu\text{mol}\cdot\text{m}^{-2}\cdot\text{s}^{-1}$)	T + 1	0.85 (16.44)	0.73	142.22 (30.40)	204.33
	T + 2	0.80 (11.11)	0.72	157.56 (25.36)	211.10
	T + 3	0.75 (20.97)	0.62	172.89 (27.46)	238.35

¹ Forecast output at 50–60 min ahead. ² Forecast output at 110–120 min ahead. ³ Forecast output at 170–180 min ahead. ⁴ Value in parentheses denotes the improvement rate (%) of CLSTM-CNN-BP over CNN-LSTM-SLSTM-BP ($= \frac{\text{CLSTM-CNN-BP} - \text{CNN-LSTM-SLSTM-BP}}{\text{CNN-LSTM-SLSTM-BP}} \times 100\%$).

For both models, PAR achieves the highest R^2 values, followed by RH and Temp. In terms of Temp, CLSTM-CNN-BP outperforms CNN-LSTM-SLSTM-BP in R^2 and RMSE at T + 1 and T + 2 horizons, as CLSTM-CNN-BP includes an additional input: simulated internal greenhouse Temp (T + 1–T + 3) from a physics-based model. However, the accuracy of the physics-based model decreases over time, making it more beneficial for short-term than long-term forecasts. For RH, further analysis shows CNN-LSTM-SLSTM-BP slightly surpasses CLSTM-CNN-BP in R^2 and RMSE for RH across T + 1 to T + 3, due to the nonlinear relationship between Temp and RH, despite CLSTM-CNN-BP's use of internal Temp data. Notably, CLSTM-CNN-BP shows a more significant improvement in R^2 than in RMSE for PAR over CNN-LSTM-SLSTM-BP, which is explained by the low ratio of the mean to the standard deviation for internal PAR (0.69), indicating that the mean is

much lower than the standard deviation, which poses challenges with regard to accurately forecasting peak PAR values.

In summary, the proposed CLSTM-CNN-BP model achieves comparable forecast accuracy to the benchmark model (CNN-LSTM-SLSTM-BP) that incorporates the greenhouse's external IoT data while also providing enhanced noise reduction and superior feature extraction. This advancement represents a significant milestone in the development of accessible and cost-effective microclimate forecast solutions for precision agriculture.

3.4. Development of an AI-Enabled Greenhouse Environmental Control Module

In this study, the TARI greenhouse is equipped with an external shading net on the roof, two rolling plastic films that open the roof skylights, and four plastic films around the perimeter, each of which is controlled by independent motors and connected to the greenhouse control system. Based on the five steps outlined previously, we develop an AI-enabled environmental control module (see Figure 7a).

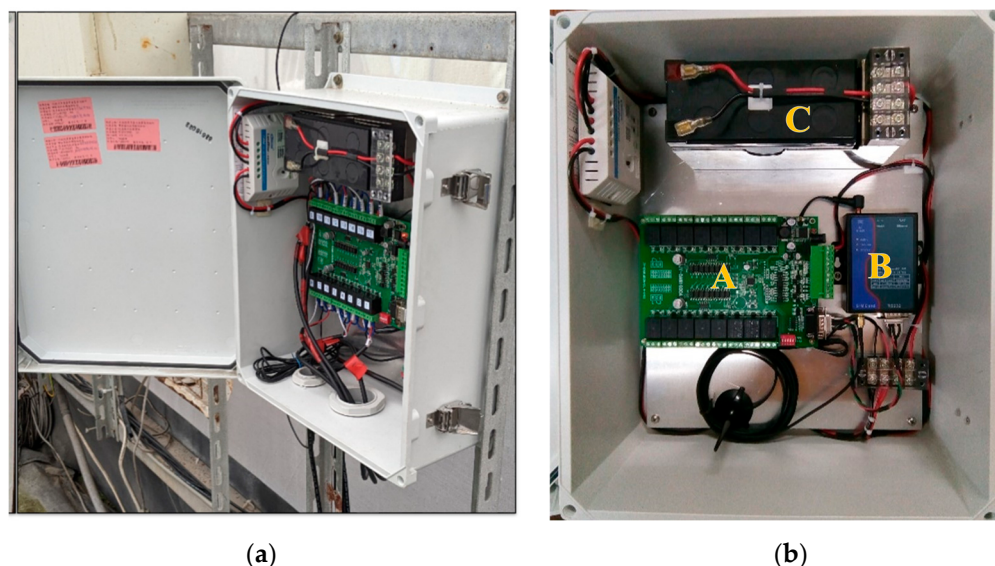


Figure 7. AI-enabled environmental control module. (a) Module size: 39 cm × 34 cm × 17.5 cm. (b) A: Relay control board; B: network sub-module; and C: backup battery (12 V).

Part A of Figure 7b displays the relay control board, which comprises 16 segments and 8 switches. This board is responsible for executing command codes received from the remote server, thereby managing the operation of eight greenhouse devices: the left- and right-side skylights, the left and right lower and upper rollers, the back roller, and the external shading net.

Part B of Figure 7b shows the network sub-module, which establishes a connection to the remote server through 4G. This sub-module enables the reception of AI-generated decisions and facilitates the transmission of commands to the control board, ensuring seamless communication and operational efficiency.

Part C of Figure 7b illustrates the backup battery (12 V). Given the potential for sudden power outages in the greenhouse, this external battery serves a dual purpose: it provides backup power during outages and absorbs voltage spikes that may occur upon power restoration, thereby protecting the equipment within the control module from potential damage.

This integrated approach not only enhances the operational capabilities of the greenhouse but also ensures resilience against power interruptions, thereby promoting more reliable and effective environmental control for optimal crop growth.

4. Discussion, Limitations, and Future Research

The design and modules of the AI-GECS are original, with no directly comparable research in the existing literature. Developed based on the specific needs of farmers and the agricultural industry, the system addresses key business and operational challenges that have been identified in previous studies and reports. Traditional greenhouse IoT technologies often rely on extensive sensor deployment [16,17], enabling accurate microclimate monitoring but raising concerns regarding high investment costs and operational complexity. For instance, farmers may struggle to recover costs associated with IoT deployment, frequent malfunctions, and system maintenance. In addition, many systems require specialized staff for effective operation, further increasing operational burdens. To overcome these challenges, the proposed AI-GECS was designed with cost efficiency and ease of use in mind. It significantly reduces sensor deployment costs while incorporating AI-driven forecasting capabilities. The system uses publicly available grid-based meteorological data to generate optimal greenhouse control commands through AI computations. This allows environmental control equipment to operate proactively, reducing adverse crop growth conditions without requiring expensive or complex infrastructure. Unlike traditional systems, the hardware in the greenhouse only needs to execute simple commands to operate cooling or shading equipment. As a result, the AI-GECS offers a user-friendly solution at roughly one-tenth the cost of conventional greenhouse environmental control systems. This makes it a scalable, practical, and economically viable option for farmers, with substantial potential for widespread adoption.

Physics-based models are highly regarded for their robust theoretical foundation and generalizability. However, they have certain limitations, including being data-intensive, complex to develop and calibrate, computationally demanding, sensitive to assumptions, and limited in their adaptability to poorly understood or highly variable systems. These limitations indicate the need for hybrid approaches that combine physics-based models with AI to leverage their strengths while addressing their weaknesses. To this end, our proposed AI-GECS integrates simulated internal temperature data from a physics-based model (Equation (3)) into a hybrid deep learning forecast model (CLSTM-CNN-BP). This integration enables accurate microclimate forecasting within greenhouses for up to three hours while reducing reliance on costly IoT devices. By combining the precision of physics-based simulations with the adaptability of AI, this approach provides an innovative and cost-effective solution for precision agriculture.

To investigate the practicability of the proposed AI-GECS, a greenhouse operation period (from 23 October to 26 October 2020) was selected. Figure 8 presents the operation results based on the forecasts from the CLSTM-CNN-BP model for the TARI greenhouse, where greenhouse operation consider (a) the impact of environmental control equipment on the microclimate and (b) the photosynthesis rate at a $T + 1$ horizon (one hour ahead). The results indicate that the trends for Temp and RH are effectively captured (Figure 8a,b). The proposed CLSTM-CNN-BP demonstrates satisfactory performance in forecasting Temp (Figure 8a); however, it tends to underestimate RH (Figure 8b). This underestimation can be attributed to the narrow observed Temp range, which allows the model to easily capture peak values. In contrast, the broader range of observed RH reflects greater variability, presenting a challenge for the model to accurately forecast peak RH values.

The model also shows commendable performance in forecasting PAR, adequately capturing peak values. High R^2 values (0.84) are observed between the forecasted and actual data, as illustrated in Figure 8c. Despite this, the forecast errors for PAR are relatively substantial ($RMSE = 112.9 \mu\text{mol}\cdot\text{m}^{-2}\cdot\text{s}^{-1}$) compared to the mean values in the observed dataset ($97.39 \mu\text{mol}\cdot\text{m}^{-2}\cdot\text{s}^{-1}$).

The proposed AI-GECS can seamlessly integrate with existing agricultural systems, such as weather and climate information services [55] and agricultural disaster prevention systems [41], to enhance natural disaster warning capabilities. By forecasting conditions like heavy rainfall or low temperatures and coupling these forecasts with the AI-driven environmental control module of the AI-GECS, this integration can empower smallholder

farmers to adopt protected cultivation practices. Such a synergy minimizes crop losses, enhances resilience to adverse weather conditions, and promotes sustainable agricultural practices. Moreover, weather and climate conditions play a crucial role in crop development, influencing phenological stages, disease risks, and crop quality [56]. This study highlights the potential of the AI-GECS to integrate with crop management practices, enabling a resource-efficient production process and optimizing the use of water and fertilizers while ensuring effective and sustainable farming outcomes.

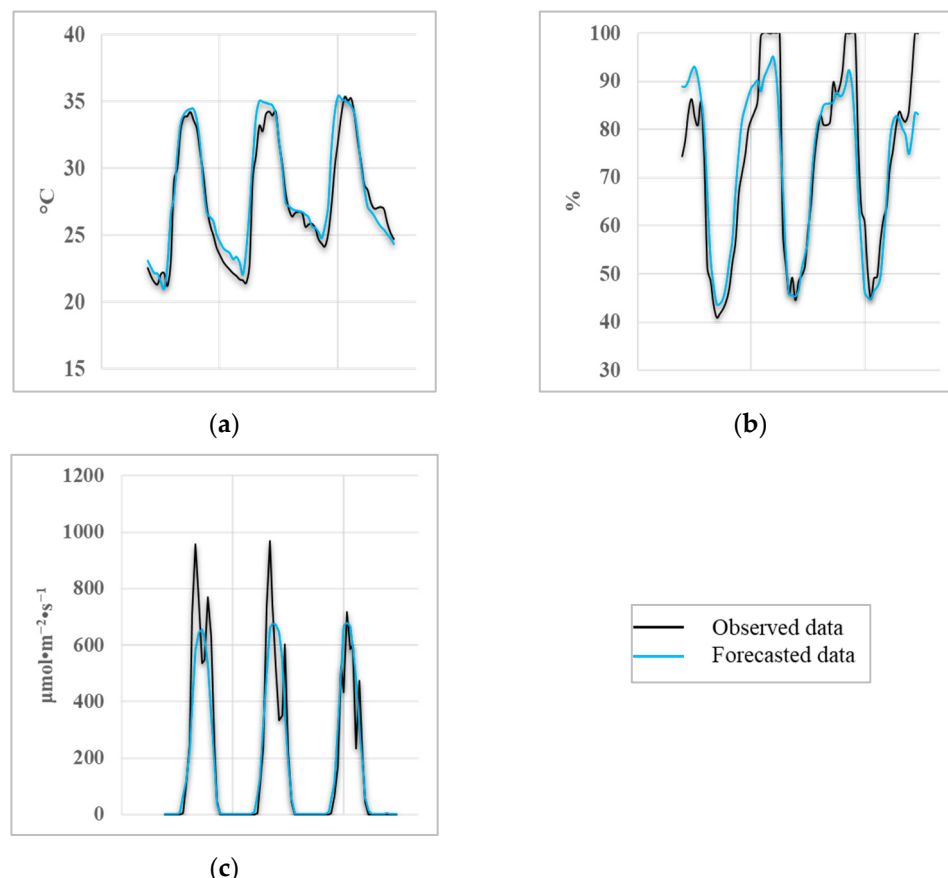


Figure 8. The performance of the proposed AI-GECS implemented in the TARI greenhouse during 9 October 2020 and 12 October 2020. Microclimate forecasts at $T + 1$ were generated from CLSTM-CNN-BP in consideration of the impact of environmental control equipment on microclimate and photosynthesis rate. (a) Internal Temp ($^{\circ}\text{C}$); (b) internal RH (%); (c) internal PAR ($\mu\text{mol}\cdot\text{m}^{-2}\cdot\text{s}^{-1}$).

4.1. Limitation

The microclimate forecasts generated by the CLSTM-CNN-BP model within the AI-GECS reveal certain limitations encountered during the research. For Temp, forecast errors primarily stem from uncertainties in the gridded weather dataset and the quality of greenhouse control data. For RH, significant sources of error include terrain variability, the distance between the greenhouse and weather monitoring stations, and the quality of IoT data. For PAR, forecast errors are largely due to the absence of cloud density information. While these forecasts are not entirely free of error, they provide sufficient accuracy to support the development and operation of climate-smart greenhouses, demonstrating the potential of AI-GECS in advancing precision agriculture.

4.2. Future Research

The proposed AI-GECS seamlessly integrates four key modules—refined gridded weather forecasts, microclimate forecasts, crop physiological indicator, and environmental

control—within a cloud-based architecture. This integration increases the greenhouse's operational capabilities, ensuring resilience against power interruptions and promoting more reliable, effective environmental control for optimal crop growth. The framework and methodology of the AI-GECS are designed to be scalable and transferable, making them applicable to a variety of greenhouse and agricultural environments.

Future research could focus on enhancing the system's adaptability to accommodate a broader range of greenhouse structures and agricultural settings, further advancing its role in promoting sustainable and efficient farming practices. We also recommend exploring the integration of additional crop physiological indicators to optimize yields while reducing water and fertilizer usage. Such advancements could lead to smarter, more resource-efficient greenhouse management, paving the way for broader applications and greater contributions to precision agriculture.

5. Conclusions

This study introduces a groundbreaking greenhouse control system, the AI-powered greenhouse environmental control system (AI-GECS), which is designed to optimize environmental management in agricultural settings. The AI-GECS operates through a series of innovative steps: first, it transforms 3 h gridded weather forecast data into hourly forecasts using a Multi-Model Super Ensemble (MMSE) system based on the STMAS-WRF-IDW model for effective downscaling. Next, it employs a hybrid deep learning model, CLSTM-CNN-BP, to accurately predict changes in the greenhouse microclimate, leveraging the refined hourly gridded forecast data.

The system then adjusts the predicted microclimate data by considering the interactions between different control equipment configurations and the greenhouse environment. Finally, the adjusted data are fed into a photosynthesis model, from which the configuration that maximizes the photosynthesis rate is selected to guide the environmental control measures for the following hour. This dynamic control process is executed hourly, allowing the system to proactively activate cooling or rain protection measures, thereby enhancing crop growth conditions.

The proposed AI-GECS contributes significantly to scientific advancements in greenhouse management by addressing cost and operational challenges associated with traditional systems. A key innovation lies in its cloud-based architecture. It reduces sensor deployment costs while incorporating advanced forecasting capabilities, enabling proactive operation of environmental control equipment. By utilizing open-source grid-based meteorological data provided by public agencies and generating optimal control commands through AI-driven microclimate forecasts, the system eliminates the need for costly and complex IoT setups. The greenhouse hardware simply executes commands to operate cooling or shading equipment, making the system user-friendly and approximately one-tenth the cost of conventional greenhouse environmental control systems—from approximately USD 10,000 to USD 15,000 for traditional systems to a mere USD 1000 to USD 1700. This scalability and affordability position the AI-GECS as a practical solution with significant potential for widespread adoption.

Author Contributions: Conceptualization, M.-H.L., M.-H.Y., F.-J.C. and P.-Y.K.; methodology, M.-H.L., M.-H.Y. and P.-Y.K.; and software, M.-H.L. and P.-Y.K.; validation, M.-H.Y. and P.-Y.K.; formal analysis, M.-H.L., M.-H.Y. and P.-Y.K.; investigation, M.-H.Y.; resources, M.-H.Y. and B.-J.K.; data curation, P.-Y.K.; writing—original draft preparation, M.-H.L.; writing—review and editing, F.-J.C.; visualization, P.-Y.K.; supervision, M.-H.Y. and B.-J.K.; project administration, M.-H.Y. and F.-J.C.; funding acquisition, F.-J.C. and M.-H.Y. All authors have read and agreed to the published version of the manuscript.

Funding: This research was funded by the National Science and Technology Council, Taiwan, grant numbers 110-2321-B-055-001-; 112-2621-M-002-019-; and 113-2621-M-002-017-.

Institutional Review Board Statement: Not applicable.

Informed Consent Statement: Not applicable.

Data Availability Statement: Data are available from the corresponding authors upon reasonable request.

Acknowledgments: The datasets provided by the Central Weather Administration in Taiwan and the Taiwan Agricultural Research Institute are acknowledged. The authors also extend their sincere appreciation to the Editors and anonymous Reviewers for their valuable and constructive feedback, which has significantly enhanced the quality and depth of the article.

Conflicts of Interest: The authors declare no conflicts of interest.

References

1. Yu, M.; Liu, X.; Li, Q. Responses of meteorological drought-hydrological drought propagation to watershed scales in the upper Huaihe River basin, China. *Environ. Sci. Pollut. Res.* **2020**, *27*, 17561–17570.
2. Chen, T.H.; Lee, M.H.; Hsia, I.W.; Hsu, C.H.; Yao, M.H.; Chang, F.J. Develop a smart microclimate control system for greenhouses through system dynamics and machine learning techniques. *Water* **2022**, *14*, 3941. [[CrossRef](#)]
3. Sun, W.; Chang, F.J. Empowering greenhouse cultivation: Dynamic factors and machine learning unite for advanced microclimate prediction. *Water* **2023**, *15*, 3548. [[CrossRef](#)]
4. Zhang, P.; Li, M.; Fu, Q.; Singh, V.P.; Du, C.; Liu, D.; Li, T.; Yang, A. Dynamic regulation of the irrigation–nitrogen–biochar nexus for the synergy of yield, quality, carbon emission and resource use efficiency in tomato. *J. Integr. Agric.* **2024**, *23*, 680–697. [[CrossRef](#)]
5. Boursianis, A.D.; Papadopoulou, M.S.; Gotsis, A.; Wan, S.; Sarigiannidis, P.; Nikolaidis, S.; Goudos, S.K. Smart Irrigation System for Precision Agriculture-The AREThOU5A IoT Platform. *IEEE Sens. J.* **2020**, *21*, 17539–17547.
6. Liu, L.W.; Ma, X.; Wang, Y.M.; Lu, C.T.; Lin, W.S. Using artificial intelligence algorithms to predict rice (*Oryza sativa* L.) growth rate for precision agriculture. *Comput. Electron. Agric.* **2021**, *187*, 106286.
7. Aznar-Sánchez, J.A.; Velasco-Muñoz, J.F.; López-Felices, B.; Román-Sánchez, I.M. An analysis of global research trends on greenhouse technology: Towards a sustainable agriculture. *Int. J. Environ. Res. Public Health* **2020**, *17*, 664. [[CrossRef](#)]
8. Baddadi, S.; Bouadila, S.; Ghorbel, W.; Guizani, A. Autonomous greenhouse microclimate through hydroponic design and refurbished thermal energy by phase change material. *J. Clean. Prod.* **2019**, *211*, 360–379. [[CrossRef](#)]
9. Ahmed, H.A.; Tong, Y.X.; Yang, Q.C.; Al-Faraj, A.A.; Abdel-Ghany, A.M. Spatial distribution of air temperature and relative humidity in the greenhouse as affected by external shading in arid climates. *J. Integr. Agric.* **2019**, *18*, 2869–2882.
10. Nicola, S.; Pignata, G.; Ferrante, A.; Bulgari, R.; Cocetta, G.; Ertani, A. Water use efficiency in greenhouse systems and its application in horticulture. *AgroLife Sci. J.* **2020**, *9*, 248–262.
11. Kamienski, C.; Soininen, J.P.; Taumberger, M.; Dantas, R.; Toscano, A.; Salmon Cinotti, T.; Filev Maia, R.; Torre Neto, A. Smart water management platform: IoT-based precision irrigation for agriculture. *Sensors* **2019**, *19*, 276. [[CrossRef](#)]
12. Hemming, S.; de Zwart, F.; Elings, A.; Petropoulou, A.; Righini, I. Cherry tomato production in intelligent greenhouses-sensors and AI for control of climate, irrigation, crop yield, and quality. *Sensors* **2020**, *20*, 6430. [[CrossRef](#)]
13. Li, K.; Fang, H.; Zou, Q.R.; Cheng, R.F. Optimization of rhizosphere cooling airflow for microclimate regulation and its effects on lettuce growth in plant factory. *J. Integr. Agric.* **2021**, *20*, 2680–2695. [[CrossRef](#)]
14. Islam, M.N.; Iqbal, M.Z.; Ali, M.; Gulandaz, M.A.; Kabir, M.S.N.; Jang, S.-H.; Chung, S.-O. Evaluation of a 0.7 kW suspension-type dehumidifier module in a closed chamber and in a small greenhouse. *Sustainability* **2023**, *15*, 5236. [[CrossRef](#)]
15. Yao, M.H.; Wang, H.C.; Chiu, Y.W.; Hsieh, H.C.; Chang, T.H.; Lee, Y.J. Integrating micro-weather forecasts and crop physiological indicators for greenhouse environmental control. *Acta Hortic.* **2021**, *1327*, 445–454. [[CrossRef](#)]
16. Bhujel, A.; Basak, J.K.; Khan, F.; Arulmozhi, E.; Jaihuni, M.; Sihalath, T.; Lee, D.; Park, J.; Kim, H.T. Sensor systems for greenhouse microclimate monitoring and control: A review. *J. Biosyst. Eng.* **2020**, *45*, 341–361. [[CrossRef](#)]
17. Kirci, P.; Ozturk, E.; Celik, Y. A novel approach for monitoring of smart greenhouse and flowerpot parameters and detection of plant growth with sensors. *Agriculture* **2022**, *12*, 1705. [[CrossRef](#)]
18. Elanchezian, A.; Basak, J.K.; Park, J.; Khan, F.; Okyere, F.G.; Lee, Y.; Bhujel, A.; Lee, D.; Sihalath, T.; Kim, H.T. Evaluating different models used for predicting the indoor microclimatic parameters of a greenhouse. *Appl. Ecol. Environ. Res.* **2020**, *18*, 2141–2161. [[CrossRef](#)]
19. Petrakis, T.; Kavga, A.; Thomopoulos, V.; Argiriou, A.A. Neural network model for greenhouse microclimate predictions. *Agriculture* **2022**, *12*, 780. [[CrossRef](#)]
20. Singh, M.C.; Singh, J.P.; Singh, K.G. Development of a microclimate model for prediction of temperatures inside a naturally ventilated greenhouse under cucumber crop in soilless media. *Comput. Electron. Agric.* **2018**, *154*, 227–238. [[CrossRef](#)]
21. Kocian, A.; Massa, D.; Cannazzaro, S.; Incrocci, L.; Di Lonardo, S.; Milazzo, P.; Chessa, S. Dynamic Bayesian network for crop growth prediction in greenhouses. *Comput. Electron. Agric.* **2020**, *169*, 105167. [[CrossRef](#)]
22. Yang, H.; Liu, Q.F.; Yang, H.Q. Deterministic and stochastic modelling of greenhouse microclimate. *Syst. Sci. Control. Eng.* **2019**, *7*, 65–72. [[CrossRef](#)]
23. Liu, T.; Yuan, Q.; Wang, Y. Hierarchical optimization control based on crop growth model for greenhouse light environment. *Comput. Electron. Agric.* **2021**, *180*, 105854. [[CrossRef](#)]

24. Zhang, W.; Zhang, W.; Yang, Y.; Hu, G.; Ge, D.; Liu, H.; Cao, H. A cloud computing-based approach using the visible near-infrared spectrum to classify greenhouse tomato plants under water stress. *Comput. Electron. Agric.* **2021**, *181*, 105966.
25. Kittas, C.; Bartzanas, T. Greenhouse microclimate and dehumidification effectiveness under different ventilator configurations. *Build. Environ.* **2007**, *42*, 3774–3784. [[CrossRef](#)]
26. Benni, S.; Tassinari, P.; Bonora, F.; Barbaresi, A.; Torreggiani, D. Efficacy of greenhouse natural ventilation: Environmental monitoring and CFD simulations of a study case. *Energy Build.* **2016**, *125*, 276–286. [[CrossRef](#)]
27. Bartzanas, T.; Boulard, T.; Kittas, C. Effect of vent arrangement on windward ventilation of a tunnel greenhouse. *Biosyst. Eng.* **2004**, *88*, 479–490. [[CrossRef](#)]
28. Occhipinti, A.; Rogers, L.; Angione, C. A pipeline and comparative study of 12 machine learning models for text classification. *Expert Syst. Appl.* **2022**, *201*, 117193. [[CrossRef](#)]
29. Xu, T.; Yao, L.; Xu, L.; Chen, Q.; Yang, Z. Image segmentation of cucumber seedlings based on genetic algorithm. *Sustainability* **2023**, *15*, 3089. [[CrossRef](#)]
30. Hemming, S.; de Zwart, F.; Elings, A.; Righini, I.; Petropoulou, A. Remote control of greenhouse vegetable production with artificial intelligence—Greenhouse climate, irrigation, and crop production. *Sensors* **2019**, *19*, 1807. [[CrossRef](#)]
31. Kow, P.Y.; Lu, M.K.; Lee, M.H.; Lu, W.B.; Chang, F.J. Develop a hybrid machine learning model for promoting microbe biomass production. *Bioresour. Technol.* **2023**, *369*, 128412. [[CrossRef](#)]
32. Qu, Y.; Clausen, A.; Jørgensen, B.N. Application of deep neural network on net photosynthesis modeling. In Proceedings of the 2021 IEEE 19th International Conference on Industrial Informatics (INDIN), Palma de Mallorca, Spain, 21–23 July 2021; pp. 1–7.
33. Choab, N.; Allouhi, A.; El Maakoul, A.; Kousksou, T.; Saadeddine, S.; Jamil, A. Review on greenhouse microclimate and application: Design parameters, thermal modeling and simulation, climate controlling technologies. *Solar Energy* **2019**, *191*, 109–137. [[CrossRef](#)]
34. Hernández-Salazar, J.A.; Hernández-Rodríguez, D.; Hernández-Cruz, R.A.; Ramos-Fernández, J.C.; Márquez-Vera, M.A.; Trejo-Macotela, F.R. Estimation of the evapotranspiration using ANFIS algorithm for agricultural production in greenhouse. In Proceedings of the 2019 IEEE International Conference on Applied Science and Advanced Technology (iCASAT), Queretaro, Mexico, 27–28 November 2019; pp. 1–5.
35. Jung, D.H.; Kim, H.S.; Jhin, C.; Kim, H.J.; Park, S.H. Time-serial analysis of deep neural network models for prediction of climatic conditions inside a greenhouse. *Comput. Electron. Agric.* **2020**, *173*, 105402. [[CrossRef](#)]
36. Jung, D.-H.; Lee, T.S.; Kim, K.; Park, S.H. A deep learning model to predict evapotranspiration and relative humidity for moisture control in tomato greenhouses. *Agronomy* **2022**, *12*, 2169. [[CrossRef](#)]
37. Ajani, O.S.; Usigbe, M.J.; Aboyeji, E.; Uyeh, D.D.; Ha, Y.; Park, T.; Mallipeddi, R. Greenhouse micro-climate prediction based on fixed sensor placements: A machine learning approach. *Mathematics* **2023**, *11*, 3052. [[CrossRef](#)]
38. Shamshiri, R.R.; Bojic, I.; van Henten, E.; Balasundram, S.K.; Dworak, V.; Sultan, M.; Weltzien, C. Model-based evaluation of greenhouse microclimate using IoT-Sensor data fusion for energy-efficient crop production. *J. Clean. Prod.* **2020**, *263*, 121303. [[CrossRef](#)]
39. Li, H.; Guo, Y.; Zhao, H.; Wang, Y.; Chow, D. Towards automated greenhouse: A state of the art review on greenhouse monitoring methods and technologies based on internet of things. *Comput. Electron. Agric.* **2021**, *191*, 106558. [[CrossRef](#)]
40. Saddik, A.; Latif, R.; Taher, F.; El Ouardi, A.; Elhoseny, M. Mapping agricultural soil in greenhouse using an autonomous low-cost robot and precise monitoring. *Sustainability* **2022**, *14*, 15539. [[CrossRef](#)]
41. Yao, M.H.; Hsu, Y.H.; Li, T.Y.; Chen, Y.M.; Lu, C.T.; Chen, C.L.; Shih, P.Y. Agricultural disaster prevention system: Insights from Taiwan’s adaptation strategies. *Atmosphere* **2024**, *15*, 526. [[CrossRef](#)]
42. Peng, J.; Xie, Y.; Kang, Z.; Li, H. Application of an improved radar data assimilation scheme in heavy rain forecast in Meiyu Period. *Plateau Meteorol.* **2020**, *39*, 1007–1022.
43. Dall’Agnol, R.W.; Michelon, G.K.; Bazzi, C.L.; Magalhães, P.S.G.; de Souza, E.G.; Betzek, N.M.; Sobjak, R. Web applications for spatial analyses and thematic map generation. *Comput. Electron. Agric.* **2020**, *172*, 105374.
44. Mueller, T.G.; Pusuluri, N.B.; Mathias, K.K.; Cornelius, P.L.; Barnhisel, R.I.; Shearer, S.A. Map quality for ordinary kriging and inverse distance weighted interpolation. *Soil Sci. Soc. Am. J.* **2004**, *68*, 2042–2047.
45. Krishnamurti, T.N.; Kishtawal, C.M.; Shin, D.W.; Williford, C.E. Improving tropical precipitation forecasts from a multianalysis superensemble. *J. Clim.* **2000**, *13*, 4218–4227.
46. Kim, H.; Jung, W.K.; Park, Y.C.; Lee, J.W.; Ahn, S.H. Broken stitch detection method for sewing operation using CNN feature map and image-processing techniques. *Expert Syst. Appl.* **2022**, *188*, 116014.
47. Kow, P.Y.; Hsia, I.W.; Chang, L.C.; Chang, F.J. Real-time image-based air quality estimation by deep learning neural networks. *J. Environ. Manag.* **2022**, *307*, 114560. [[PubMed](#)]
48. Kao, I.F.; Liou, J.Y.; Lee, M.H.; Chang, F.J. Fusing stacked autoencoder and long short-term memory for regional multistep-ahead flood inundation forecasts. *J. Hydrol.* **2021**, *598*, 126371.
49. Vukovic, D.B.; Romanyuk, K.; Ivashchenko, S.; Grigorieva, E.M. Are CDS spreads predictable during the Covid-19 pandemic? Forecasting based on SVM, GMDH, LSTM and Markov switching autoregression. *Expert Syst. Appl.* **2022**, *194*, 116553. [[PubMed](#)]
50. Hsu, C.H. Predict Indoor Environment of Greenhouses for Automatic Greenhouse Environmental Control Using Machine Learning Techniques. Master’s Thesis, Institute of Bio-Environmental Systems Engineering, National Taiwan University, Taipei, Taiwan, 2020.

51. Boote, K.J.; Pickering, N.B. Modeling photosynthesis of row crop canopies. *HortScience* **1994**, *29*, 1423–1434.
52. Boote, K.J.; Rybak, M.R.; Scholberg, J.M.S.; Jones, J.W. Improving the CROPGRO-Tomato model for predicting growth and yield response to temperature. *HortScience* **2012**, *47*, 1038–1049.
53. Johnson, I.R.; Thornley, J.H.M. Temperature dependence of plant and crop processes. *Ann. Bot.* **1985**, *5*, 1.
54. Evans, J.R.; Farquhar, G.D. Modelling canopy photosynthesis from the biochemistry of the C₃ chloroplast. In *Modelling Crop Photosynthesis: From Biochemistry to Canopy*; Boote, K.J., Loomis, R.S., Eds.; Crop Science Society of America: Madison, WI, USA, 1991; pp. 1–15.
55. Sutanto, S.J.; Paparrizos, S.; Kumar, U.; Datta, D.K.; Ludwig, F. The performance of Climate Information Service in delivering scientific, local, and hybrid weather forecasts: A study case in Bangladesh. *Clim. Serv.* **2024**, *34*, 100459. [[CrossRef](#)]
56. Perez-Zanon, N.; Agudetse, V.; Baulenas, E.; Bretonniere, P.A.; Delgado-Torres, C.; Gonzalez-Reviriego, N.; Manrique-Sunen, A.; Nicodemou, A.; Olid, M.; Palma Ll Terrado, M.; et al. Lessons learned from the co-development of operational climate forecast services for vineyards management. *Clim. Serv.* **2024**, *36*, 100513. [[CrossRef](#)]

Disclaimer/Publisher’s Note: The statements, opinions and data contained in all publications are solely those of the individual author(s) and contributor(s) and not of MDPI and/or the editor(s). MDPI and/or the editor(s) disclaim responsibility for any injury to people or property resulting from any ideas, methods, instructions or products referred to in the content.